BABAR-CONF-02/13
SLAC-PUB-9304
hep-ex/0207065
July 2002

Measurements of Branching Fractions and Direct *CP* Asymmetries in $\pi^+\pi^0$, $K^+\pi^0$ and $K^0\pi^0$ B Decays

The *BABAR* Collaboration

July 24, 2002

Abstract

We present preliminary results of the analyses of $B^+ \to h^+\pi^0$ (with $h^+ = \pi^+, K^+$) and $B^0 \to K^0\pi^0$ decays from a sample of approximately 88 million $B\overline{B}$ pairs collected by the *BABAR* detector at the PEP-II asymmetric-energy B Factory at SLAC. We measure the $\pi^+\pi^0$ branching fraction and we obtain

$$\mathcal{B}(B^+ \to \pi^+\pi^0) = (5.5^{+1.0}_{-0.9} \pm 0.6) \times 10^{-6}$$

with a significance of 7.7σ including systematic uncertainties. We measure the $K^+\pi^0$ and $K^0\pi^0$ branching fractions to be $\mathcal{B}(B^+ \to K^+\pi^0) = (12.8^{+1.2}_{-1.1} \pm 1.0) \times 10^{-6}$ and $\mathcal{B}(B^0 \to K^0\pi^0) = (10.4 \pm 1.5 \pm 0.8) \times 10^{-6}$. At the same time, the direct *CP*-violating asymmetries are investigated and we find $\mathcal{A}_{\pi^+\pi^0} = -0.03^{+0.18}_{-0.17} \pm 0.02$, $\mathcal{A}_{K^+\pi^0} = -0.09 \pm 0.09 \pm 0.01$ and $\mathcal{A}_{K^0\pi^0} = 0.03 \pm 0.36 \pm 0.09$, where the errors are statistical and systematic, respectively.

Contributed to the 31^{st} International Conference of High Energy Physics,
7/24-7/31/2002, Amsterdam, The Netherlands

Stanford Linear Accelerator Center, Stanford University, Stanford, CA 94309

Work supported in part by Department of Energy contract DE-AC03-76SF00515.

The *BABAR* Collaboration,

B. Aubert, D. Boutigny, J.-M. Gaillard, A. Hicheur, Y. Karyotakis, J. P. Lees, P. Robbe, V. Tisserand, A. Zghiche

Laboratoire de Physique des Particules, F-74941 Annecy-le-Vieux, France

A. Palano, A. Pompili

Università di Bari, Dipartimento di Fisica and INFN, I-70126 Bari, Italy

J. C. Chen, N. D. Qi, G. Rong, P. Wang, Y. S. Zhu

Institute of High Energy Physics, Beijing 100039, China

G. Eigen, I. Ofte, B. Stugu

University of Bergen, Inst. of Physics, N-5007 Bergen, Norway

G. S. Abrams, A. W. Borgland, A. B. Breon, D. N. Brown, J. Button-Shafer, R. N. Cahn, E. Charles, M. S. Gill, A. V. Gritsan, Y. Groysman, R. G. Jacobsen, R. W. Kadel, J. Kadyk, L. T. Kerth, Yu. G. Kolomensky, J. F. Kral, C. LeClerc, M. E. Levi, G. Lynch, L. M. Mir, P. J. Oddone, T. J. Orimoto, M. Pripstein, N. A. Roe, A. Romosan, M. T. Ronan, V. G. Shelkov, A. V. Telnov, W. A. Wenzel

Lawrence Berkeley National Laboratory and University of California, Berkeley, CA 94720, USA

T. J. Harrison, C. M. Hawkes, D. J. Knowles, S. W. O'Neale, R. C. Penny, A. T. Watson, N. K. Watson

University of Birmingham, Birmingham, B15 2TT, United Kingdom

T. Deppermann, K. Goetzen, H. Koch, B. Lewandowski, K. Peters, H. Schmuecker, M. Steinke

Ruhr Universität Bochum, Institut für Experimentalphysik 1, D-44780 Bochum, Germany

N. R. Barlow, W. Bhimji, J. T. Boyd, N. Chevalier, P. J. Clark, W. N. Cottingham, C. Mackay, F. F. Wilson

University of Bristol, Bristol BS8 1TL, United Kingdom

K. Abe, C. Hearty, T. S. Mattison, J. A. McKenna, D. Thiessen

University of British Columbia, Vancouver, BC, Canada V6T 1Z1

S. Jolly, A. K. McKemey

Brunel University, Uxbridge, Middlesex UB8 3PH, United Kingdom

V. E. Blinov, A. D. Bukin, A. R. Buzykaev, V. B. Golubev, V. N. Ivanchenko, A. A. Korol, E. A. Kravchenko, A. P. Onuchin, S. I. Serednyakov, Yu. I. Skovpen, A. N. Yushkov

Budker Institute of Nuclear Physics, Novosibirsk 630090, Russia

D. Best, M. Chao, D. Kirkby, A. J. Lankford, M. Mandelkern, S. McMahon, D. P. Stoker

University of California at Irvine, Irvine, CA 92697, USA

C. Buchanan, S. Chun

University of California at Los Angeles, Los Angeles, CA 90024, USA

H. K. Hadavand, E. J. Hill, D. B. MacFarlane, H. Paar, S. Prell, Sh. Rahatlou, G. Raven, U. Schwanke, V. Sharma

University of California at San Diego, La Jolla, CA 92093, USA

J. W. Berryhill, C. Campagnari, B. Dahmes, P. A. Hart, N. Kuznetsova, S. L. Levy, O. Long, A. Lu, M. A. Mazur, J. D. Richman, W. Verkerke

University of California at Santa Barbara, Santa Barbara, CA 93106, USA

J. Beringer, A. M. Eisner, M. Grothe, C. A. Heusch, W. S. Lockman, T. Pulliam, T. Schalk, R. E. Schmitz, B. A. Schumm, A. Seiden, M. Turri, W. Walkowiak, D. C. Williams, M. G. Wilson

University of California at Santa Cruz, Institute for Particle Physics, Santa Cruz, CA 95064, USA

E. Chen, G. P. Dubois-Felsmann, A. Dvoretskii, D. G. Hitlin, F. C. Porter, A. Ryd, A. Samuel, S. Yang

California Institute of Technology, Pasadena, CA 91125, USA

S. Jayatilleke, G. Mancinelli, B. T. Meadows, M. D. Sokoloff

University of Cincinnati, Cincinnati, OH 45221, USA

T. Barillari, P. Bloom, W. T. Ford, U. Nauenberg, A. Olivas, P. Rankin, J. Roy, J. G. Smith, W. C. van Hoek, L. Zhang

University of Colorado, Boulder, CO 80309, USA

J. L. Harton, T. Hu, M. Krishnamurthy, A. Soffer, W. H. Toki, R. J. Wilson, J. Zhang

Colorado State University, Fort Collins, CO 80523, USA

D. Altenburg, T. Brandt, J. Brose, T. Colberg, M. Dickopp, R. S. Dubitzky, A. Hauke, E. Maly, R. Müller-Pfefferkorn, S. Otto, K. R. Schubert, R. Schwierz, B. Spaan, L. Wilden

Technische Universität Dresden, Institut für Kern- und Teilchenphysik, D-01062 Dresden, Germany

D. Bernard, G. R. Bonneaud, F. Brochard, J. Cohen-Tanugi, S. Ferrag, S. T'Jampens, Ch. Thiebaux, G. Vasileiadis, M. Verderi

Ecole Polytechnique, LLR, F-91128 Palaiseau, France

A. Anjomshoaa, R. Bernet, A. Khan, D. Lavin, F. Muheim, S. Playfer, J. E. Swain, J. Tinslay

University of Edinburgh, Edinburgh EH9 3JZ, United Kingdom

M. Falbo

Elon University, Elon University, NC 27244-2010, USA

C. Borean, C. Bozzi, L. Piemontese, A. Sarti

Università di Ferrara, Dipartimento di Fisica and INFN, I-44100 Ferrara, Italy

E. Treadwell

Florida A&M University, Tallahassee, FL 32307, USA

F. Anulli,[1] R. Baldini-Ferroli, A. Calcaterra, R. de Sangro, D. Falciai, G. Finocchiaro, P. Patteri, I. M. Peruzzi,[1] M. Piccolo, A. Zallo

Laboratori Nazionali di Frascati dell'INFN, I-00044 Frascati, Italy

S. Bagnasco, A. Buzzo, R. Contri, G. Crosetti, M. Lo Vetere, M. Macri, M. R. Monge, S. Passaggio, F. C. Pastore, C. Patrignani, E. Robutti, A. Santroni, S. Tosi

Università di Genova, Dipartimento di Fisica and INFN, I-16146 Genova, Italy

[1]Also with Università di Perugia, I-06100 Perugia, Italy

S. Bailey, M. Morii

Harvard University, Cambridge, MA 02138, USA

R. Bartoldus, G. J. Grenier, U. Mallik

University of Iowa, Iowa City, IA 52242, USA

J. Cochran, H. B. Crawley, J. Lamsa, W. T. Meyer, E. I. Rosenberg, J. Yi

Iowa State University, Ames, IA 50011-3160, USA

M. Davier, G. Grosdidier, A. Höcker, H. M. Lacker, S. Laplace, F. Le Diberder, V. Lepeltier, A. M. Lutz, T. C. Petersen, S. Plaszczynski, M. H. Schune, L. Tantot, S. Trincaz-Duvoid, G. Wormser

Laboratoire de l'Accélérateur Linéaire, F-91898 Orsay, France

R. M. Bionta, V. Brigljević , D. J. Lange, K. van Bibber, D. M. Wright

Lawrence Livermore National Laboratory, Livermore, CA 94550, USA

A. J. Bevan, J. R. Fry, E. Gabathuler, R. Gamet, M. George, M. Kay, D. J. Payne, R. J. Sloane, C. Touramanis

University of Liverpool, Liverpool L69 3BX, United Kingdom

M. L. Aspinwall, D. A. Bowerman, P. D. Dauncey, U. Egede, I. Eschrich, G. W. Morton, J. A. Nash, P. Sanders, D. Smith, G. P. Taylor

University of London, Imperial College, London, SW7 2BW, United Kingdom

J. J. Back, G. Bellodi, P. Dixon, P. F. Harrison, R. J. L. Potter, H. W. Shorthouse, P. Strother, P. B. Vidal

Queen Mary, University of London, E1 4NS, United Kingdom

G. Cowan, H. U. Flaecher, S. George, M. G. Green, A. Kurup, C. E. Marker, T. R. McMahon, S. Ricciardi, F. Salvatore, G. Vaitsas, M. A. Winter

University of London, Royal Holloway and Bedford New College, Egham, Surrey TW20 0EX, United Kingdom

D. Brown, C. L. Davis

University of Louisville, Louisville, KY 40292, USA

J. Allison, R. J. Barlow, A. C. Forti, F. Jackson, G. D. Lafferty, A. J. Lyon, N. Savvas, J. H. Weatherall, J. C. Williams

University of Manchester, Manchester M13 9PL, United Kingdom

A. Farbin, A. Jawahery, V. Lillard, D. A. Roberts, J. R. Schieck

University of Maryland, College Park, MD 20742, USA

G. Blaylock, C. Dallapiccola, K. T. Flood, S. S. Hertzbach, R. Kofler, V. B. Koptchev, T. B. Moore, H. Staengle, S. Willocq

University of Massachusetts, Amherst, MA 01003, USA

B. Brau, R. Cowan, G. Sciolla, F. Taylor, R. K. Yamamoto

Massachusetts Institute of Technology, Laboratory for Nuclear Science, Cambridge, MA 02139, USA

M. Milek, P. M. Patel

McGill University, Montréal, QC, Canada H3A 2T8

F. Palombo

Università di Milano, Dipartimento di Fisica and INFN, I-20133 Milano, Italy

J. M. Bauer, L. Cremaldi, V. Eschenburg, R. Kroeger, J. Reidy, D. A. Sanders, D. J. Summers

University of Mississippi, University, MS 38677, USA

C. Hast, P. Taras

Université de Montréal, Laboratoire René J. A. Lévesque, Montréal, QC, Canada H3C 3J7

H. Nicholson

Mount Holyoke College, South Hadley, MA 01075, USA

C. Cartaro, N. Cavallo, G. De Nardo, F. Fabozzi, C. Gatto, L. Lista, P. Paolucci, D. Piccolo, C. Sciacca

Università di Napoli Federico II, Dipartimento di Scienze Fisiche and INFN, I-80126, Napoli, Italy

J. M. LoSecco

University of Notre Dame, Notre Dame, IN 46556, USA

J. R. G. Alsmiller, T. A. Gabriel

Oak Ridge National Laboratory, Oak Ridge, TN 37831, USA

J. Brau, R. Frey, M. Iwasaki, C. T. Potter, N. B. Sinev, D. Strom, E. Torrence

University of Oregon, Eugene, OR 97403, USA

F. Colecchia, A. Dorigo, F. Galeazzi, M. Margoni, M. Morandin, M. Posocco, M. Rotondo, F. Simonetto, R. Stroili, C. Voci

Università di Padova, Dipartimento di Fisica and INFN, I-35131 Padova, Italy

M. Benayoun, H. Briand, J. Chauveau, P. David, Ch. de la Vaissière, L. Del Buono, O. Hamon, Ph. Leruste, J. Ocariz, M. Pivk, L. Roos, J. Stark

Universités Paris VI et VII, Lab de Physique Nucléaire H. E., F-75252 Paris, France

P. F. Manfredi, V. Re, V. Speziali

Università di Pavia, Dipartimento di Elettronica and INFN, I-27100 Pavia, Italy

L. Gladney, Q. H. Guo, J. Panetta

University of Pennsylvania, Philadelphia, PA 19104, USA

C. Angelini, G. Batignani, S. Bettarini, M. Bondioli, F. Bucci, G. Calderini, E. Campagna, M. Carpinelli, F. Forti, M. A. Giorgi, A. Lusiani, G. Marchiori, F. Martinez-Vidal, M. Morganti, N. Neri, E. Paoloni, M. Rama, G. Rizzo, F. Sandrelli, G. Triggiani, J. Walsh

Università di Pisa, Scuola Normale Superiore and INFN, I-56010 Pisa, Italy

M. Haire, D. Judd, K. Paick, L. Turnbull, D. E. Wagoner

Prairie View A&M University, Prairie View, TX 77446, USA

J. Albert, G. Cavoto,[2] N. Danielson, P. Elmer, C. Lu, V. Miftakov, J. Olsen, S. F. Schaffner, A. J. S. Smith, A. Tumanov, E. W. Varnes

Princeton University, Princeton, NJ 08544, USA

[2]Also with Università di Roma La Sapienza, Roma, Italy

F. Bellini, D. del Re, R. Faccini,[3] F. Ferrarotto, F. Ferroni, E. Leonardi, M. A. Mazzoni, S. Morganti, M. Pierini, G. Piredda, F. Safai Tehrani, M. Serra, C. Voena

Università di Roma La Sapienza, Dipartimento di Fisica and INFN, I-00185 Roma, Italy

S. Christ, G. Wagner, R. Waldi

Universität Rostock, D-18051 Rostock, Germany

T. Adye, N. De Groot, B. Franek, N. I. Geddes, G. P. Gopal, S. M. Xella

Rutherford Appleton Laboratory, Chilton, Didcot, Oxon, OX11 0QX, United Kingdom

R. Aleksan, S. Emery, A. Gaidot, P.-F. Giraud, G. Hamel de Monchenault, W. Kozanecki, M. Langer, G. W. London, B. Mayer, G. Schott, B. Serfass, G. Vasseur, Ch. Yeche, M. Zito

DAPNIA, Commissariat à l'Energie Atomique/Saclay, F-91191 Gif-sur-Yvette, France

M. V. Purohit, A. W. Weidemann, F. X. Yumiceva

University of South Carolina, Columbia, SC 29208, USA

I. Adam, D. Aston, N. Berger, A. M. Boyarski, M. R. Convery, D. P. Coupal, D. Dong, J. Dorfan, W. Dunwoodie, R. C. Field, T. Glanzman, S. J. Gowdy, E. Grauges , T. Haas, T. Hadig, V. Halyo, T. Himel, T. Hryn'ova, M. E. Huffer, W. R. Innes, C. P. Jessop, M. H. Kelsey, P. Kim, M. L. Kocian, U. Langenegger, D. W. G. S. Leith, S. Luitz, V. Luth, H. L. Lynch, H. Marsiske, S. Menke, R. Messner, D. R. Muller, C. P. O'Grady, V. E. Ozcan, A. Perazzo, M. Perl, S. Petrak, H. Quinn, B. N. Ratcliff, S. H. Robertson, A. Roodman, A. A. Salnikov, T. Schietinger, R. H. Schindler, J. Schwiening, G. Simi, A. Snyder, A. Soha, S. M. Spanier, J. Stelzer, D. Su, M. K. Sullivan, H. A. Tanaka, J. Va'vra, S. R. Wagner, M. Weaver, A. J. R. Weinstein, W. J. Wisniewski, D. H. Wright, C. C. Young

Stanford Linear Accelerator Center, Stanford, CA 94309, USA

P. R. Burchat, C. H. Cheng, T. I. Meyer, C. Roat

Stanford University, Stanford, CA 94305-4060, USA

R. Henderson

TRIUMF, Vancouver, BC, Canada V6T 2A3

W. Bugg, H. Cohn

University of Tennessee, Knoxville, TN 37996, USA

J. M. Izen, I. Kitayama, X. C. Lou

University of Texas at Dallas, Richardson, TX 75083, USA

F. Bianchi, M. Bona, D. Gamba

Università di Torino, Dipartimento di Fisica Sperimentale and INFN, I-10125 Torino, Italy

L. Bosisio, G. Della Ricca, S. Dittongo, L. Lanceri, P. Poropat, L. Vitale, G. Vuagnin

Università di Trieste, Dipartimento di Fisica and INFN, I-34127 Trieste, Italy

R. S. Panvini

Vanderbilt University, Nashville, TN 37235, USA

[3]Also with University of California at San Diego, La Jolla, CA 92093, USA

S. W. Banerjee, C. M. Brown, D. Fortin, P. D. Jackson, R. Kowalewski, J. M. Roney

University of Victoria, Victoria, BC, Canada V8W 3P6

H. R. Band, S. Dasu, M. Datta, A. M. Eichenbaum, H. Hu, J. R. Johnson, R. Liu, F. Di Lodovico, A. Mohapatra, Y. Pan, R. Prepost, I. J. Scott, S. J. Sekula, J. H. von Wimmersperg-Toeller, J. Wu, S. L. Wu, Z. Yu

University of Wisconsin, Madison, WI 53706, USA

H. Neal

Yale University, New Haven, CT 06511, USA

1 Introduction

The study of B meson decays into charmless hadronic final states plays an important role in the understanding of *CP* violation in the B system. Measurements of the *CP*-violating asymmetry in the $\pi^+\pi^-$ decay mode can provide information on the angle α of the Unitarity Triangle. However, in contrast to the theoretically clean determination of the angle β in B decays to charmonium final states [1, 2] the extraction of α from $\pi^+\pi^-$ decays is complicated by the interference of $b \to uW^-$ tree and $b \to dg$ penguin amplitudes. Since these amplitudes have similar magnitude but carry different weak phases, additional measurements of the isospin-related decays[1], $B^+ \to \pi^+\pi^0$ and $B^0 \to \pi^0\pi^0$, are required to provide a way of measuring the angle α [3]. The measurement of the branching fraction of the $B^+ \to \pi^+\pi^0$ decay is, in fact, a crucial ingredient, since it is a pure tree decay to a very good approximation. Therefore, in this channel direct *CP* violation, detected as a charge asymmetry ($\mathcal{A}_{\pi^+\pi^0}$), is expected to be zero.

On the other hand, measurements of $B \to K\pi$ decays can be related to a model dependent extraction of the weak phase γ with a global fit to the observables. In order to do this, several models have been proposed, based on different dynamical assumptions for B decays to two light pseudoscalar mesons [4–7]. All these approaches are able to reproduce experimental values for branching fractions, but they do not show a good sensitivity to the value of the weak phase γ. Providing information on *CP*-violating asymmetries could contribute to increase this sensitivity, clarifying the theoretical framework and improving our ability to constrain the Unitarity Triangle in the $(\bar{\rho}, \bar{\eta})$ plane [8].

In the case of $K^0\pi^0$, the ideal measurement is a time dependent analysis of the $K^0_S\pi^0$ final state, which is a *CP* eigenstate. In this way, one would be sensitive to the direct *CP*-violating asymmetry (related to the coefficient of the cosine term) and to the weak phase entering the decay (related to the coefficient of the sine term) [9]. In the present analysis, we perform a time integrated study, providing the direct *CP*-violating asymmetry defined as

$$\mathcal{A}_{CP} = \frac{|\overline{A}|^2 - |A|^2}{|\overline{A}|^2 + |A|^2},$$

where A ($\overline{A}$) is the decay amplitude (its *CP* conjugated) taken into account. We actually investigate $\mathcal{A}_{K^0_S\pi^0}$ which, in the SM, is equal to $\mathcal{A}_{K^0\pi^0}$, neglecting contributions with more than one weak boson.

We present here results on the $B^+ \to \pi^+\pi^0$, $B^+ \to K^+\pi^0$ and $B^0 \to K^0\pi^0$ decays. The *BABAR* collaboration has previously published [10] observations of these channels: we now have reduced the errors on branching fractions and investigated direct *CP*-violating effects.

2 The *BABAR* Detector and Data Set

The data used in these analyses were collected with the *BABAR* detector at the PEP-II e^+e^- storage ring. The sample corresponds to an integrated luminosity of about $81\,\text{fb}^{-1}$ accumulated on the $\Upsilon(4S)$ resonance ("on-resonance") and about $9\,\text{fb}^{-1}$ accumulated at a center-of-mass (CM) energy about 40 MeV below the $\Upsilon(4S)$ resonance ("off-resonance"), which are used for background studies. The on-resonance sample corresponds to $(87.9 \pm 1.0) \times 10^6$ $B\overline{B}$ pairs. The collider is operated with asymmetric beam energies, producing a boost ($\beta\gamma = 0.55$) of the $\Upsilon(4S)$ along the collision axis.

[1] Charge conjugate modes are assumed throughout this paper unless explicitly stated.

BABAR is a solenoidal detector optimized for the asymmetric beam configuration at PEP-II and is described in detail in Ref. [11]. Charged particle (track) momenta are measured in a tracking system consisting of a 5-layer, double-sided, silicon vertex tracker and a 40-layer drift chamber filled with a gas mixture of helium and isobutane, both operating within a 1.5 T superconducting solenoidal magnet. Photon candidates are selected as local maxima of deposited energy in an electromagnetic calorimeter (EMC) consisting of 6580 CsI(Tl) crystals arranged in barrel and forward endcap subdetectors. In this analysis, tracks are identified as pions or kaons by the Cherenkov angle θ_c measured by a detector of internally reflected Cherenkov light (DIRC). The DIRC system is a unique type of Cherenkov detector that relies on total internal reflection within the radiating volumes (quartz bars) to deliver the Cherenkov light outside the tracking and magnetic volumes, where the Cherenkov ring is imaged by an array of ~ 11000 photomultiplier tubes. The Cherenkov angle θ_c is measured with a typical resolution of 3 mrad, with a separation between kaons and pions of 8σ (2.5σ) at 2 GeV/c (4 GeV/c). Good separation at high momenta is essential for two-body B decay since the boost increases the momentum range of the decay products from a narrow distribution centered near 2.6 GeV/c in the CM to a broad distribution extending from 1.7 up to 4.3 GeV/c.

3 Event Selection, π^0 and K^0 Reconstruction

Hadronic events are selected based on track multiplicity and event topology. Backgrounds from non-hadronic events are reduced by requiring the ratio of the second to zeroth Fox-Wolfram moment [12] to be less than 0.95 and the sphericity [13] of the event to be greater than 0.01.

Charged π and K candidates (except for K^0_S daughters) are reconstructed within the tracking fiducial volume and quality criteria are imposed: they are required to originate within 1.5 cm in the xy plane and 10 cm in z from the interaction point, to have at least 12 measured drift chamber hits and a minimum transverse momentum of 0.1 GeV/c.

Candidate π^0 mesons are reconstructed as pairs of photons with an invariant mass within 3σ of the nominal π^0 mass [14], where the resolution σ is about 8 MeV/c^2. Photon candidates are selected as showers in the EMC that have the expected lateral shape, are not matched to a charged track, and have a minimum energy of 30 MeV. The π^0 candidates are then kinematically fitted with their mass constrained to the π^0 nominal mass.

K^0 mesons are detected in the mode $K^0 \to K^0_S \to \pi^+\pi^-$. K^0_S candidates are reconstructed from pairs of oppositely charged tracks that form a well-measured vertex and have an invariant mass within 11.2 MeV/c^2 (which corresponds to 3.5σ) of the nominal K^0_S mass [14]. The measured proper decay time of the K^0_S candidate is required to exceed 5 times its uncertainty.

4 B Reconstruction

Charged (neutral) B meson candidates are reconstructed by combining a π^0 candidate with a track h^+ (a K^0_S candidate). The kinematic constraints provided by the $\Upsilon(4S)$ initial state and knowledge of the beam energies are exploited to efficiently identify B candidates. We define a beam-energy substituted mass $m_{\rm ES} = \sqrt{E^2_{\rm b} - \mathbf{p}^2_B}$, where $E_{\rm b} = (s/2 + \mathbf{p}_i \cdot \mathbf{p}_B)/E_i$, $\sqrt{s}$ and E_i are the total energies of the e^+e^- system in the CM and lab frames, respectively, and $\mathbf{p}_i$ and $\mathbf{p}_B$ are the momentum vectors in the lab frame of the e^+e^- system and the B candidate, respectively. An additional kinematic parameter ΔE is defined as the difference between the energy of the B candidate and

half the energy of the e^+e^- system, computed in the CM system. The $m_{\rm ES}$ resolution is dominated by the beam energy spread, while for ΔE the main contribution comes from the measurement of particle energies in the detector. These two variables are therefore substantially uncorrelated ($\leq 6\%$).

For all the decay modes, the signal energy-substituted mass is parameterized on simulated signal events by a Crystal Ball[2] function. The resolution is found to be about 2.9 MeV/c^2 and it is validated by comparing data and Monte Carlo resolutions for decays into open charm final states with large branching fractions, such as $B^- \to D^0\rho^-$, (with $\rho^- \to \pi^-\pi^0$ and $D^0 \to K^-\pi^+$).

The ΔE distribution for the signal $h^+\pi^0$ and $K^0\pi^0$ events is described by another Crystal Ball function. The mean value of this distribution is directly obtained from the fit for the $h^+\pi^0$ sample and assumed to be the same for $K^0\pi^0$ since the dominant effect comes from the π^0 energy scale. For $K^+\pi^0$ candidates, the mean of ΔE is also shifted because the pion mass is assumed for all charged tracks in order to extract the yields of both modes and the ΔE mean from one fit. This shifted mean value can be expressed as

$$\langle \Delta E \rangle = -\gamma_{\rm boost} \times \left(\sqrt{M_K^2 + p^2} - \sqrt{M_\pi^2 + p^2} \right) ,$$

where p is the momentum of the assumed kaon track, and M_π and M_K are the pion and kaon mass values, respectively. We estimate the resolution on ΔE to be about 42 MeV, based on simulated $B^+ \to h^+\pi^0$ and $B^0 \to K^0_S\pi^0$ events and cross-checked on the $B^- \to D^0\rho^-$ control sample.

Candidates are selected in the range $5.2 < m_{\rm ES} < 5.3\,{\rm GeV}/c^2$. Different requirements on ΔE specific to each analysis are described later.

5 Background Rejection

The dominant background to these channels is the continuum background, coming from random combinations of a true π^0 with a track (a true K^0_S), produced in $e^+e^- \to q\overline{q}$ continuum events (where $q = u$, d, s or c). Another source of background originates from B decays into other light charmless meson final states (charmless background). The main contribution to this background comes from $B^+ \to \rho^+\pi^0$ and $B^0 \to \rho^\pm\pi^\mp$ in the case of $B^+ \to \pi^+\pi^0$ and $B^+ \to K^{*+}\pi^0$ in the case of $B^+ \to K^+\pi^0$ and $B^0 \to K^0\pi^0$. Detailed Monte Carlo simulation, off-resonance, and on-resonance data are used to study backgrounds.

In the CM frame the continuum background typically exhibits a two-jet structure, in contrast to the isotropic decay of $B\overline{B}$ pairs produced in $\Upsilon(4S)$ decays. We exploit the topology difference between signal and background by making use of two event-shape quantities. The first variable is the angle θ_S between the sphericity axes of the B candidate and of the remaining tracks and photons in the event. The distribution of $|\cos\theta_S|$ in the CM frame is strongly peaked near 1 for continuum events and is approximately uniform for $B\overline{B}$ events. We require $|\cos\theta_S| < 0.8$. The second quantity is a Fisher discriminant $\mathcal{F}$, constructed from the quantities L_0 and L_2, where L_j is:

$$L_j = \sum_i p_i |\cos\theta_i|^j$$

and p_i (θ_i) is the momentum (the angle with respect to the thrust axis of the B candidate in the CM frame) of each charged track and neutral cluster not used to reconstruct the candidate B meson.

[2]The Crystal Ball function [15] is a core Gaussian with a power law to describe the left tail.

Monte Carlo samples are used to obtain the values of the Fisher coefficients, which are determined by maximizing the statistical separation between signal and background events. No requirement is applied on $\mathcal{F}$; instead the distributions for signal and background events are included in a maximum likelihood fit as described in the next section.

On the other hand, charmless background events tend to peak in $m_{\rm ES}$, as do signal events, and have the same $\mathcal{F}$ distribution as signal, since they are true B decays. Nevertheless they are characterized by lower ΔE values, since at least a pion is lost in the B reconstruction. A cut on ΔE is the only way to reduce this background to a negligible level. We use on-resonance data in the negative ΔE sideband region ($-0.40 < \Delta E < -0.20\,\mathrm{GeV}$) to estimate the magnitude of this background. The efficiency determined from Monte Carlo events is used to scale the number of events in the sidebands and get the expected number of events in the chosen signal region. We finally require $-0.11 < \Delta E < 0.15\,\mathrm{GeV}$ for $h^+\pi^0$ and $-0.15 < \Delta E < 0.15\,\mathrm{GeV}$ for $K^0\pi^0$, reducing the charmless background contribution to the level of less than 1%.

A total of 21752 candidates in the on-resonance data satisfy the $h^+\pi^0$ selection, and a total of 2668 candidates satisfy the $K^0_S\pi^0$ selection. These two samples enter into two separate maximum likelihood fits.

The final signal selection efficiency ϵ is (26.1±1.7)% for $B^+ \to \pi^+\pi^0$ and (21.5±1.5)% for $B^+ \to K^+\pi^0$ events, while it is $(28.0 \pm 2.0)\%$ for $B^0 \to K^0_S\pi^0$ events. The errors on the efficiencies are statistical and systematic, combined in quadrature. The dominant contribution to the systematic error is due to the imperfect knowledge of π^0 and K^0_S reconstruction efficiencies (5% and 3% relative errors, respectively). The hierarchy of efficiency values comes from the difference in ΔE lower cut ($h^+\pi^0$ vs. $K^0_S\pi^0$) and from the use of the π mass hypothesis in the ΔE calculation ($\pi^+\pi^0$ vs. $K^+\pi^0$).

6 Signal Extraction

For each topology ($h^+\pi^0$ and $K^0\pi^0$), an unbinned maximum likelihood fit determines the signal and background yields n_i ($i = 1$ to M, where M is the total number of signal and background types) and *CP* asymmetries. The measured asymmetry is defined as:

$$\mathcal{A}^i_m = \frac{\bar{n}_i - n_i}{\bar{n}_i + n_i}$$

where $\bar{n}_i$ is the fitted number of i^{th} type $h^-\pi^0$ [$\overline{K}^0\pi^0$] events and n_i corresponds to $h^+\pi^0$ [$K^0\pi^0$] events. The input variables ($\vec{x}_j$) to the fit are $m_{\rm ES}$, ΔE, $\mathcal{F}$ and, in the case of charged modes, the Cherenkov angle θ_c of the track from the candidate B decay to distinguish between the final states with $h = \pi$ and $h = K$.

The $h^+\pi^0$ extended likelihood function $\mathcal{L}$ is defined as

$$\mathcal{L} = \exp\left(-\sum_{i=1}^{M} n_i\right) \prod_{j=1}^{N} \left[\sum_{i=1}^{M} \frac{1}{2}(1 - q_j\mathcal{A}^i_m) n_i \mathcal{P}_i\left(\vec{x}_j;\vec{\alpha}_i\right)\right],$$

where q_j is the charge of the track h in the j^{th} event and, in this case, M is equal to 4 including signal and background $\pi^+\pi^0$ and $K^+\pi^0$. The M probabilities $\mathcal{P}_i(\vec{x}_j;\vec{\alpha}_i)$ are evaluated as the product of probability density functions (PDFs) for each of the independent variables $\vec{x}_j$, given the set of parameters $\vec{\alpha}_i$ which define the PDF shapes. Monte Carlo simulation is used to validate

the assumption that the fit variables are uncorrelated. The exponential factor in the likelihood accounts for Poisson fluctuations in the total number of observed events N.

For the $K^0\pi^0$ mode we need to measure the flavor of the B candidate in order to extract the CP asymmetry. We use B flavor tagging information to distinguish B^0 from $\overline{B}^0$ decays. B candidates are defined B^0 when the other B is recognized to be a $\overline{B}^0$ and vice versa. Details of *BABAR* B flavor tagging can be found in Ref. [9]. We have four different tagging categories ($k = 1, .., 4$), with different tagging efficiencies ϵ^k and wrong tag fractions w^k. We also use untagged events ($k = 0$) in the fit. The extended likelihood is

$$\mathcal{L} = \exp\left(-\sum_{i=1}^{M} n_i\right) \prod_{j=1}^{N} \left[\sum_{k=0}^{4}\sum_{i=1}^{M} \frac{1}{2}\delta(c_j - k)(1 - f_j(1 - 2w^k)\mathcal{A}_m^i) n_i^k \mathcal{P}_i^k\left(\vec{x}_j; \vec{\alpha}_{i_k}\right)\right],$$

where c_j and f_j are the tagging category and the measured flavor of the j^{th} event, $n_i^k = \epsilon^k n_i$ is the number of events of the i^{th} type in the k^{th} category and M, in this case, is equal to 2 including signal and background. The $\mathcal{P}_i^k(\vec{x}_j; \vec{\alpha}_{i_k})$ are in principle category dependent. We found that such dependence can be ignored without any bias in the fit, for all the PDFs, except for background $m_{\rm ES}$ and background $\mathcal{F}$.

The $m_{\rm ES}$ shape in background is parameterized by the ARGUS threshold function [16]

$$f(x) \propto x\sqrt{1 - x^2}\exp[-\xi(1 - x^2)]$$

where $x = m_{\rm ES}/m_0$ and m_0 is the average CM beam energy, and ξ is the parameter determining the shape of the distribution and is left free to float in the likelihood fits. The background shape in ΔE is parameterized as a second-order polynomial whose coefficients are taken from a fit to the on-resonance $m_{\rm ES}$ sideband region. The signal distributions have been already described in Sect. 4.

Events from simulated signal decays and from on-resonance $m_{\rm ES}$ sideband regions are used to parameterize the Fisher discriminant PDFs for signal and background events as a bifurcated Gaussian[3] and a sum of two Gaussians, respectively. Alternative parameterizations for $\mathcal{F}$, obtained from off-resonance data (for background) and from a large sample of fully reconstructed $B^0 \to D^{(*)}n\pi$ decays (for signal), are used to estimate systematic uncertainties. The θ_c PDFs are derived from kaon and pion tracks in the momentum range of interest from a sample of $D^{*+} \to D^0\pi^+$ ($D^0 \to K^-\pi^+$) decays. This control sample is used to parameterize the θ_c resolution (σ_{θ_c}) as a function of track polar angle; double-Gaussian PDFs are constructed from the difference between measured and expected values of θ_c for the pion or kaon hypothesis, normalized by the error σ_{θ_c}. Tagging efficiencies and mistag fractions are estimated from a sample of fully reconstructed B decays.

The results of the fit are summarized in the first column of Table 1, where the statistical error for each mode corresponds to a 68% confidence level interval and is given by the change in signal yield n_i that corresponds to a $-2\ln\mathcal{L}$ increase of one unit. In the case of the $\pi^+\pi^0$ final state, we evaluate how the imperfect knowledge of the PDF shapes can affect the significance of the signal. We recalculate the square root of the change in $-2\ln\mathcal{L}$ with $n_{\pi^+\pi^0}$ fixed to zero for the worst case PDF variations and we find a statistical significance of 7.7σ for the signal.

In order to increase the relative fraction of signal events of a given type for display purpose we choose events passing requirements on probability ratios. These probability ratios are defined

[3]The bifurcated Gaussian is an asymmetric Gaussian having two different σ, one for $x > \mu$ and another for $x < \mu$, where μ is the mean value.

as $\mathcal{R}_{\rm sig} = \sum_s \mathcal{P}_s / \sum_i \mathcal{P}_i$ and $\mathcal{R}_k = \mathcal{P}_k / \sum_s \mathcal{P}_s$, where $\sum_s$ denotes the sum over the probabilities for signal hypotheses only, $\sum_i$ denotes the sum over all the probabilities (signal and background), and $\mathcal{P}_k$ denotes the probability for signal hypothesis $K^+\pi^0$ (for $h^+\pi^0$ only). These probabilities are constructed from all the PDFs except that describing the plotted variable. Figures 1 show the distributions in $m_{\rm ES}$ and ΔE for events passing all such selection criteria. The likelihood fit projections, scaled by the relative efficiencies for the probability ratio requirements, are overlaid on each distribution. Since the sample projections in $m_{\rm ES}$ and ΔE are obtained with requirements on different probability ratios, the number of signal events appearing in the two projections are not the same. The efficiencies for the $m_{\rm ES}$ plots are: 24%, 53% and 65% for $\pi^+\pi^0$, $K^+\pi^0$ and $K^0\pi^0$ signal events, respectively. For $h^+\pi^0$ ΔE projection plots, we show a wider window ($-0.200 < \Delta E < 0.150\,{\rm GeV}$) with respect to the signal region used in the maximum likelihood fit ($-0.110 < \Delta E < 0.150\,{\rm GeV}$) in order to show the $B\overline{B}$ background present at low ΔE values. The efficiencies for the ΔE plots are: 35%, 48% and 98% for $\pi^+\pi^0$, $K^+\pi^0$ and $K^0\pi^0$ signal events, respectively.

7 Branching Fraction and Direct *CP* Asymmetry Results

The branching fractions are defined as

$$\begin{aligned}
\mathcal{B}(h^+\pi^0) &= \frac{1}{\mathcal{B}(\pi^0\to\gamma\gamma)}\frac{n_{h^+\pi^0}}{\epsilon_{h^+\pi^0}\cdot N_{B\overline{B}}}, \\
\mathcal{B}(K^0\pi^0) &= \frac{n_{K^0_S\pi^0}}{\mathcal{B}(\pi^0\to\gamma\gamma)\cdot\mathcal{B}(K^0\to K^0_S)\cdot\mathcal{B}(K^0_S\to\pi^+\pi^-)\cdot\epsilon_{K^0_S\pi^0}\cdot N_{B\overline{B}}},
\end{aligned}$$

where $n_{h^+\pi^0}$ ($n_{K^0_S\pi^0}$) is the signal yield from the fit and $\epsilon_{h^+\pi^0}$ ($\epsilon_{K^0_S\pi^0}$) is the reconstruction efficiency for the mode $h^+\pi^0$ ($K^0\pi^0$) in the detected π^0 (K^0) decay chain. $N_{B\overline{B}} = (87.9 \pm 1.0)\times 10^6$ is the total number of $B\overline{B}$ pairs in our dataset. $\mathcal{B}(\pi^0\to\gamma\gamma)$, $\mathcal{B}(K^0\to K^0_S)$, and $\mathcal{B}(K^0_S\to\pi^+\pi^-)$ are taken to be equal to 0.9880, 0.5 and 0.686, respectively [14]. Implicit in the above equations is the assumption of equal branching fractions for $\Upsilon(4S)\to B^0\overline{B}^0$ and $\Upsilon(4S)\to B^+B^-$.

The *CP* asymmetry in the $K^0\pi^0$ channel is defined as:

$$\mathcal{A}_i = \mathcal{A}^i_m \cdot (1 + x_d^2)$$

where $x_d = \Delta m_d/\Gamma = 0.755 \pm 0.015$ [14]. Since the flavor of the signal B cannot be determined, we apply the correction factor $(1 + x_d^2)$ to take into account the $B^0 - \overline{B}^0$ mixing and to translate the measured asymmetry into the direct *CP* asymmetry $\mathcal{A}_{CP}$ ignoring *CP*-violating effects in mixing. In the case of the charged B, $\mathcal{A}_{h^+\pi^0} = \mathcal{A}^{h^+\pi^0}_m$. Table 1 summarizes the results on the branching fractions and the *CP* asymmetries: the 90% confidence level (CL) intervals for the asymmetries are also given.

Systematic uncertainties on the branching fractions arise primarily from uncertainty on the final selection efficiency and uncertainty on n_i due to imperfect knowledge of the PDF shapes. The latter is estimated either by varying the PDF parameters within 1σ of their measured uncertainties or by substituting alternative PDFs from independent control samples. For $K^0\pi^0$ analysis, mistag fractions and tagging efficiencies are varied by 1σ of their measured uncertainties.

In the $h^+\pi^0$ analysis the most relevant systematic uncertainties on the signal yields are due to the Fisher shape for both signal and background events (about 5% each), while for the $K^0\pi^0$ analysis the ΔE background and Fisher signal shapes contribute with the largest errors. We estimate the systematic uncertainty on the signal yields due to the residual presence of charmless

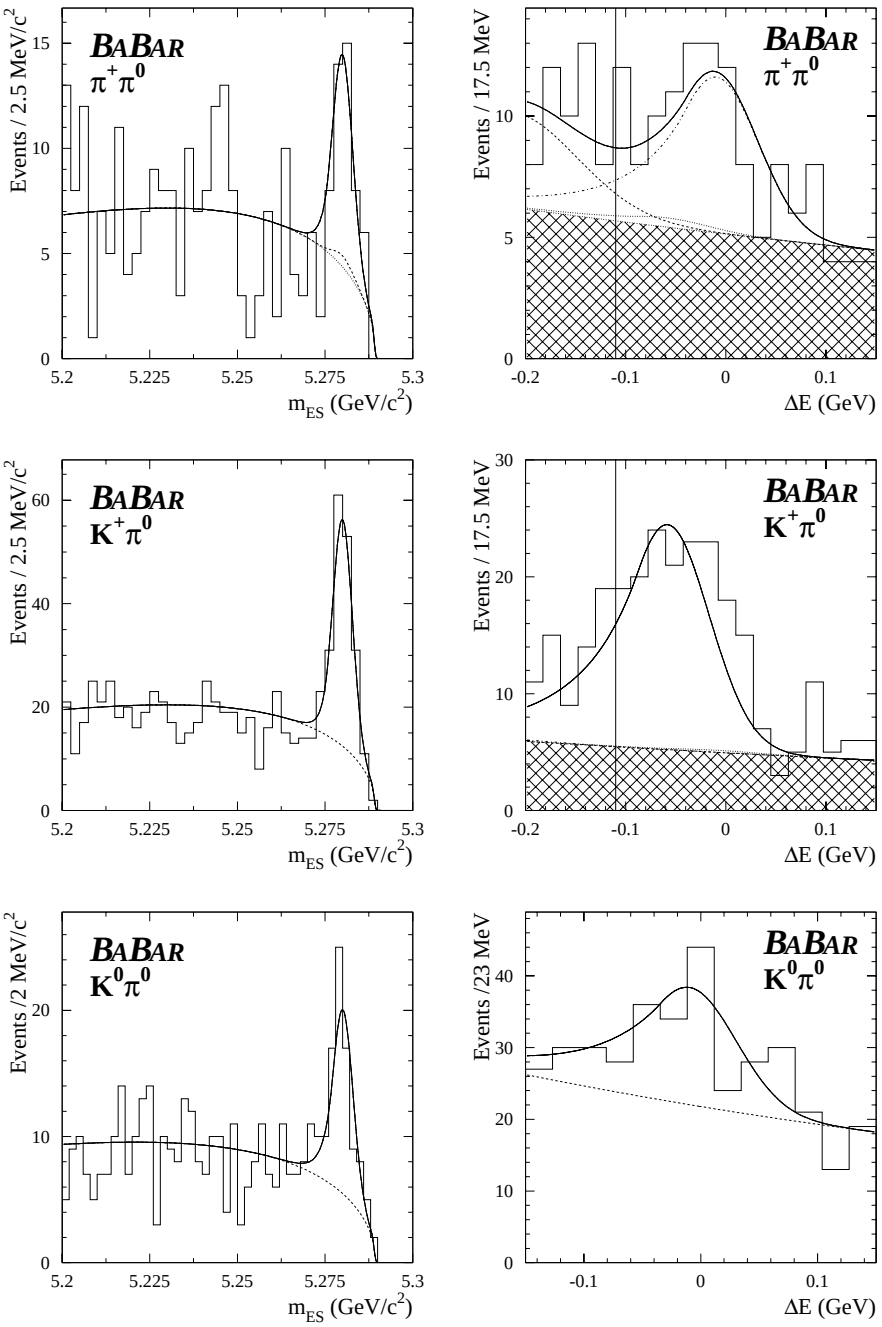

Figure 1: Distributions of $m_{\rm ES}$ (left) and ΔE (right) for $\pi^+\pi^0$ events (top), $K^+\pi^0$ events (center) and $K^0\pi^0$ events (bottom), after additional requirements on probability ratios, based on all variables except the one being plotted. Solid curves represent projections of the complete maximum likelihood fit result; dotted curves represent the background contribution. For the $m_{\rm ES}$ $\pi^+\pi^0$ plot, $K^+\pi^0$ cross-feed is also shown with a dashed curve. For ΔE $\pi^+\pi^0$ ($K^+\pi^0$) plots, hatched areas represent continuum background only. For the ΔE $\pi^+\pi^0$ plot, $\pi^+\pi^0$ signal, $K^+\pi^0$ cross-feed and $B\overline{B}$ background are represented by the dot-dashed, dotted and dashed curves, respectively. The $B\overline{B}$ background is clearly present at low ΔE values. The vertical line represents the ΔE requirement applied in the analysis.

Table 1: Summary of fitted signal yields, measured branching fraction $\mathcal{B}$ and *CP* asymmetries $\mathcal{A}_i$. The first error is statistical and the second is systematic.

Mode	Signal Yield	$\mathcal{B}\,(10^{-6})$	$\mathcal{A}_i$	$\mathcal{A}_i$ (90% CL)
$\pi^+\pi^0$	$125^{+23}_{-21} \pm 10$	$5.5^{+1.0}_{-0.9} \pm 0.6$	$-0.03^{+0.18}_{-0.17} \pm 0.02$	$[-0.32, 0.27]$
$K^+\pi^0$	$239^{+21}_{-22} \pm 6$	$12.8^{+1.2}_{-1.1} \pm 1.0$	$-0.09 \pm 0.09 \pm 0.01$	$[-0.24, 0.06]$
$K^0\pi^0$	$86 \pm 13 \pm 3$	$10.4 \pm 1.5 \pm 0.8$	$0.03 \pm 0.36 \pm 0.09$	$[-0.58, 0.64]$

backgrounds with toy Monte Carlo techniques and we find that it is negligible compared with the other effects.

Systematic uncertainties on the *CP* asymmetries are evaluated from PDF variations. For charged modes, this contribution is added in quadrature with the limit on intrinsic charge bias in the detector (0.01). For the $K^0\pi^0$ mode, an additional contribution (0.02) coming from tagging has been evaluated by moving the tagging parameters (efficiencies and mistag fractions) by 1σ from their nominal value.

In conclusion, we have presented preliminary measurements of the branching fractions of $B^+ \to \pi^+\pi^0$, $B^+ \to K^+\pi^0$ and $B^0 \to K^0\pi^0$. These measurements supersede our previous results. We do not observe any evidence of direct *CP* asymmetry in these channels.

8 Acknowledgements

We are grateful for the extraordinary contributions of our PEP-II colleagues in achieving the excellent luminosity and machine conditions that have made this work possible. The success of this project also relies critically on the expertise and dedication of the computing organizations that support *BABAR*. The collaborating institutions wish to thank SLAC for its support and the kind hospitality extended to them. This work is supported by the US Department of Energy and National Science Foundation, the Natural Sciences and Engineering Research Council (Canada), Institute of High Energy Physics (China), the Commissariat à l'Energie Atomique and Institut National de Physique Nucléaire et de Physique des Particules (France), the Bundesministerium für Bildung und Forschung and Deutsche Forschungsgemeinschaft (Germany), the Istituto Nazionale di Fisica Nucleare (Italy), the Research Council of Norway, the Ministry of Science and Technology of the Russian Federation, and the Particle Physics and Astronomy Research Council (United Kingdom). Individuals have received support from the A. P. Sloan Foundation, the Research Corporation, and the Alexander von Humboldt Foundation.

References

[1] *BABAR* Collaboration, B. Aubert *et al.*, Phys. Rev. Lett. **87**, 091801 (2001).

[2] Belle Collaboration, K. Abe *et al.*, Phys. Rev. Lett. **87**, 091802 (2001).

[3] M. Gronau, Phys. Rev. Lett. **65**, 3381 (1990).

[4] M. Beneke, G. Buchalla, M. Neubert, and C.T. Sachrajda, Nucl. Phys. B **606**, 245 (2001).

[5] M. Ciuchini, E. Franco, G. Martinelli, M. Pierini, and L. Silvestrini, Phys. Lett. B **515**, 33 (2001).

[6] Y.Y. Keum, H.N. Li and A.I. Sanda, Phys. Rev. D **63**, 054008 (2001).

[7] C. Isola, M. Ladisa, G. Nardulli, T.N. Pham and P. Santorelli, Phys. Rev. D **65**, 094005 (2002).

[8] M. Beneke, "Report on γ", summary talk of WGIII parallel section at the CKM Unitarity Triangle Workshop, CERN Feb 2002. http://ckm-workshop.web.cern.ch/ckm-workshop/

[9] *BABAR* Collaboration, B. Aubert *et al.*, hep-ex/0207042 (2002), submitted to Phys. Rev. Lett.

[10] *BABAR* Collaboration, B. Aubert *et al.*, Phys. Rev. Lett. **87**, 151802 (2001).

[11] *BABAR* Collaboration, B. Aubert *et al.*, Nucl. Instrum. and Methods A **479**, 1 (2002).

[12] G.C. Fox and S. Wolfram, Phys. Rev. Lett. **41**, 1581 (1978).

[13] J.D. Bjorken and S.J. Brodsky, Phys. Rev. D **1**, 1416 (1970).

[14] Particle Data Group, K. Hagiwara *et al.*, Phys. Rev. D **66**, 010001 (2002).

[15] E. Bloom and C. Peck, Ann. Rev. Nucl. and Part. Sci. **33**, 143 (1983).

[16] ARGUS Collaboration, H. Albrecht *et al.*, Z. Phys. C **48**, 543 (1990).